Applied Physics Letters

Magnetocrystalline anisotropy correlated negative anisotropic magnetoresistance in epitaxial $Fe_{30}Co_{70}$ thin films

Cite as: Appl. Phys. Lett. **118**, 042404 (2021); https://doi.org/10.1063/5.0034232
Submitted: 21 October 2020 • Accepted: 12 January 2021 • Published Online: 26 January 2021

Yu Miao, Dezheng Yang, Lei Jia, et al.

Applied Physics Letters ARTICLE scitation.org/journal/apl

Magnetocrystalline anisotropy correlated negative anisotropic magnetoresistance in epitaxial $Fe_{30}Co_{70}$ thin films

Cite as: Appl. Phys. Lett. **118**, 042404 (2021); doi: 10.1063/5.0034232
Submitted: 21 October 2020 · Accepted: 12 January 2021 ·
Published Online: 26 January 2021

View Online Export Citation CrossMark

Yu Miao, Dezheng Yang, Lei Jia, Xiaolin Li, Shuanglong Yang, Cunxu Gao,[a] and Desheng Xue[b]

AFFILIATIONS

Key Laboratory for Magnetism and Magnetic Materials of the Ministry of Education, Lanzhou University, 730000 Lanzhou, People's Republic of China

[a]Author to whom correspondence should be addressed: gaocunx@lzu.edu.cn
[b]xueds@lzu.edu.cn

ABSTRACT

We report on the magnetoresistance in different crystallographic directions of epitaxial ferromagnetic $Fe_{30}Co_{70}$ thin films with magnetization rotated in the film plane. A negative single crystal anisotropic magnetoresistance (SCAMR) is found when the current is along the easy magnetization axis [110], and the SCAMR can be tuned to the conventional positive one when the current flows along the hard magnetization axis [100]. This finding is explained comprehensively by a magnetocrystalline anisotropy (MCA) symmetry-adapted model expanded along the easy magnetization direction, with which the SCAMR can be represented as a MCA-independent conventional term $\cos 2\varphi_M$ and a series of MCA-dependent terms $\cos 2n\varphi_A$ $(n \geq 1)$. The results show that the MCA-dependent twofold term contributes to the negative SCAMR, which cannot be used as a fingerprint of the half-metallicity. Our finding provides an approach to understand and design the magnetoresistance with ferromagnets by MCA.

Since the discovery of longitudinal and transverse magnetization effects on the resistance of ferromagnetic materials founded in a rectangular polycrystalline sheet of Fe and Ni by Lord Kelvin in 1856,[1] the twofold symmetry characteristic of the anisotropic magnetoresistance (AMR) in polycrystalline ferromagnets is established.[2] Conventionally, the resistivity ρ_J in the current density **J** direction of the polycrystalline ferromagnets is represented as[3]

$$\frac{\rho_J - \rho_\perp}{\rho_\perp} = \frac{\rho_\parallel - \rho_\perp}{\rho_\perp} \cos^2\varphi_M, \tag{1}$$

where $\rho_\parallel(\rho_\perp)$ is the resistivity when the magnetization **M** is parallel (perpendicular) to **J** and φ_M is the angle of **M** from the **J** direction. In the polycrystalline ferromagnets, most of the metals and alloys exhibit a positive AMR with $\rho_\parallel - \rho_\perp > 0$,[3–5] and a negative AMR was also observed in several 3*d* metals and alloys containing Cr (Mo, Si)[6] or Ir,[7] $Co_2MnAl_{1-x}Si_x$ Heusler alloys,[8] and textured Fe_4N metallic compounds.[9] The anisotropy effect of the current direction-independent AMR is a consequence of *s*–*d* scattering with spin–orbit interaction (SOI),[10–12] which is called conventional AMR. Based on the two-current model proposed by Campbell–Fert–Pomeroy,[13,14] the effect of spin-related *s*–*d* scattering on AMR was supposed.[15–19] The sign of conventional AMR and its reversal can be reasonably understood with spin-polarized conduction states and localized *d* states with SOI. That is, when the dominant *s*–*d* scattering process was $s\uparrow\rightarrow d\downarrow$ $(s\uparrow\rightarrow d\uparrow)$ or $s\downarrow\rightarrow d\uparrow$ $(s\downarrow\rightarrow d\downarrow)$, the sign tended to be positive (negative).[20]

Magnetoresistance of single crystal Fe in the longitudinal magnetic field was studied decades later.[21] A crystallographic direction-dependent AMR resistance was observed in bulk[22,23] and thin films of traditional ferromagnetic metals,[24–28] ferrimagnetic oxides,[29] and antiferromagnetic material CuMnAs,[30] and of half-metallic alloys,[31] oxides,[32] and nitrides,[33] as well as magnetic semiconductors.[34,35] Two significant characteristics of the single crystal AMR (SCAMR), which is beyond the $\cos 2\varphi_M$ polycrystalline symmetry, are revealed clearly. One is higher order terms occur in addition to the twofold term, and the other is a phase-shift of the AMR terms exists in different crystallographic directions. A symmetry-adapted phenomenological theory of the AMR on current and magnetization orientation with respect to the crystal axes was given by Döring.[36] The SCAMR can be divided into a crystalline-independent term and a series of crystalline-dependent terms according to the symmetry of crystal.[35] For the cubic structure, the longitudinal SCAMR can be represented as[27,37]

$$\rho_J = C_0' + C_2' \cos 2\alpha_M \cos 2\alpha_J + S_2' \sin 2\alpha_M \sin 2\alpha_J + C_4' \cos 4\alpha_M + \cdots, \quad (2)$$

where C_i' $(i = 0, 2, 4, \ldots)$ and S_2' are the coefficients related to the crystal and α_J (α_M) is the angle between **J** (**M**) and the reference crystal axis. The SCAMR is frequently used to successfully describe the AMR of the single crystal,[38,39] polycrystal,[40] as well as textured 3*d*-ferromagnetic layers in sandwich.[41]

However, no bridge between *s*–*d* scattering with SOI and the symmetry-adapted phenomenological theory indicates that an insight into the nature of crystalline-dependent terms is still a challenge. For a defined SCAMR experimental result, the sign and phase of the crystalline-dependent terms can be differently described by the phenomenological theory with different reference crystal axes.[42] On the contrary, if the reference crystal axis along the current direction was selected, the phase-shift curve of the SCAMR[25,26] cannot be fitted well by the phenomenological theory with one set of coefficients. The fact indicates that the selection of the reference crystal axis should be limited rather than free. From this point, only the correct reference crystal axis selected in the expansion of the phenomenological theory, the conventional AMR resulted from the magnetization can be derived from the SCAMR in which the twofold symmetry term comes from both crystal-dependent and crystal-independent terms. Experimentally, the SCAMR with the same crystal structure revealed that the crystalline-dependent terms are related to the temperature[43–46] and composition.[47] Both the sign and symmetry changes of the SCAMR in Co_2MnGa,[48] GaMnAs[34] and $Ni_xFe_{4-x}N$[33,49] indicate that the reference crystal axis should be related to the anisotropic properties. Recently, the interface spin–orbit fields significantly change the symmetry of SCAMR in quasi-two-dimensional Fe/GaAs.[50] Considering that the SCAMR comes from *s*–*d* scattering with SOI (Refs. 10–12 and 20), and the magnetocrystalline anisotropy (MCA) originates from the SOI (Ref. 51), the SCAMR can be understood based on the symmetry of MCA rather than the crystalline symmetry. If so, the negative SCAMR can be observed in a certain crystallographic direction of ferromagnetic metal alloy, which has a well-known positive traditional AMR.

Here, we report the SCAMR of the epitaxial single crystal in different crystallographic directions of the body-centered cubic (bcc) $Fe_{30}Co_{70}$ thin films on MgO(001). It is found that the sign of SCAMR can be changed from negative to positive through the phase-shift gradually when the current is applied from the [110] to [100] direction in $Fe_{30}Co_{70}$. Considering the MCA-dependent resistivity tensor, the SCAMR can be divided into a MCA-independent term and a series of MCA-dependent terms. The former corresponds to the traditional AMR with a positive $\cos 2\varphi_M$ symmetry and that in the later terms contribute to the negative AMR. The MCA-related properties are consistent with the results of ferromagnetic resonance (FMR). These results provide ideas for researching and regulating positive and negative AMR in single crystalline magnetic metals under considering MCA.

High quality epitaxial $Fe_{30}Co_{70}$ thin films were fabricated and monitored by the *in situ* reflection high energy electron diffraction pattern (supplementary material I). A bcc structure was characterized by high resolution x-ray diffraction, and a lattice parameter of 2.851 Å is calculated by the diffraction peak at 32.5° of the $Fe_{30}Co_{70}$ (002) plane (supplementary material II). Hysteresis loops were measured at room temperature by a vibrating sample magnetometer. The easy magnetization axis (EA) and hard magnetization axis (HA) along [110] and [100] directions are determined by the remanence of about 1.0 and 0.7, respectively. Then, the thin films were patterned into a designed current-direction-dependent Hall bar by photolithography and ion beam etching techniques for electrical transport measurements. All of the Hall bars along the different crystallographic directions have a transverse width of 50 μm and a longitudinal length of 1000 μm. Both SCAMR and FMR were performed at room temperature by a physical property measurement system (PPMS) equipped with a motorized sample rotator and coplanar waveguide FMR measurement system, respectively.

In-plane hysteresis loops are shown in Fig. 1. The loop measured in the [110] direction has a reduced remanence of about 1.0, which indicates that the EA is along [110]. With the decreasing field, the loop measured in the [100] direction (hard axis) decreases almost linearly and has a reduced remanence of about 0.7, which is consistent with the in-plane coherent rotation magnetization process under cubic MCA.[26] With analyzing the loop in the [100] direction,[52] the anisotropy field of about 50 mT can be obtained.

Figure 2(a) shows the schematic diagram of the SCAMR measurement, where the current flows along the longitudinal direction of each Hall bar. The angles of magnetization **M** and the EA with respect to the current density **J** are φ_M and φ_{EA}, respectively. $\varphi_M = \beta - \alpha$, where α and β are the angles of magnetization **M** and the current **J** with respect to the applied magnetic field **H**, respectively. Figure 2(b) shows the longitudinal resistivity ρ_J with $\varphi_{EA} = 0°, 15°, 30°$, and 45° measured as a function of β in the film plane under an applied magnetic field of 6 T. The significant phase-shift appears in the $\rho_J \sim \beta$ curves when the direction of the EA changes from $\varphi_{EA} = 45°$ to $\varphi_{EA} = 0°$. It shows a typical positive SCAMR as $\mathbf{J} \parallel [100]$ at $\varphi_{EA} = 45°$, which is the characteristic of traditional 3*d* magnetic metal. However, the negative SCAMR as $\mathbf{J} \parallel [110]$ at $\varphi_{EA} = 0°$ occurs. Those curves with phase-shift obviously cannot be described by the conventional AMR as shown in Eq. (1).

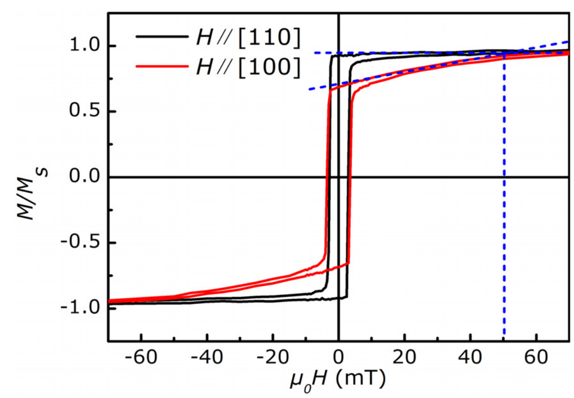

FIG. 1. Hysteresis loops with the applied magnetic field in [110] (black line) and [100] (red line) crystallographic directions.

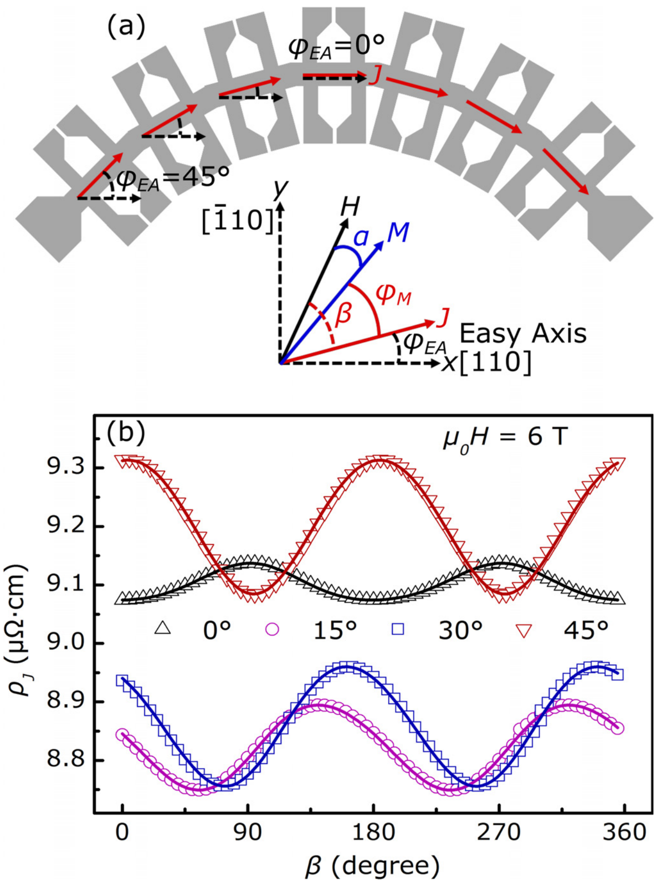

FIG. 2. (a) Measurement schematic of the SCAMR. (b) SCAMR as a function of β in the film plane under 6 T in different current directions with respect to the EA. The dots are the experimental data. The solid lines are the fitted curves by Eq. (3).

When the EA is selected as the reference crystal axis, the SCAMR in the (001) crystal plane of the bcc structure by the same process of the phenomenological theory[35,36,42] can be represented as

$$\rho_J(\varphi_M,\varphi_{EA}) = \rho_0 + \rho_2\cos 2\varphi_M + \rho_2^C \cos 2(2\varphi_{EA}+\varphi_M) + \rho_4^C \cos 4(\varphi_{EA}+\varphi_M) + \cdots, \quad (3)$$

where $\rho_0 = C_0'$, $\rho_2 = (C_2'+S_2')/2$, $\rho_2^C = (C_2'-S_2')/2$, $\rho_4^C = C_4'$ compared with Eq. (2). ρ_2, ρ_2^C, ρ_4^C are expressed as the noncrystalline AMR, crossed noncrystalline/crystalline, and cubic crystalline coefficients (Refs. 35 and 53), respectively. It clearly shows that the second term is MCA-independent, which represents the conventional AMR. The terms higher than the second term are MCA-dependent, which reveal the main difference of SCAMR from the conventional AMR and will disappear as the MCA is averaged out in polycrystalline.

Certainly, the resistivity ρ_J with $\varphi_{EA} = 0°, 15°, 30°$, and $45°$ shown in Fig. 2(b) can be well-fitted with Eq. (3) when the applied magnetic field is high enough to satisfy $\varphi_M = \beta$, where $\rho_2 = 4.185 \times 10^{-2}\ \mu\Omega$ cm and $\rho_2^C = -7.337 \times 10^{-2}\ \mu\Omega$ cm. The fitting process is similar to other reference crystal axes.[3,37,42] However, three aspects are significant when we select the EA as the reference crystal axis rather than the arbitrary crystallographic direction. First, it is reasonable in mathematics. If we regard the reference crystal axis as the current direction, Eq. (2) will be $\rho_J(\varphi_M, 0°) = C_0' + C_2'\cos 2\varphi_M + C_4'\cos 4\varphi_M + \cdots$. This means there cannot be any phase-shift when **J** is applied along the reference axis, which is not the case as shown in Fig. 2(b). Second, it is more reasonable in physics. The coefficients of Eq. (3) obtained from any one of curves shown in Fig. 2(b) can be used to fit others well. The last is the selection of the EA as the reference axis constructs the connection between the phenomenological theory and the SOI. Equation (3) is obtained by the expansion of $\rho_{ij}(\hat{\mathbf{M}})$, which is quite similar to that of the free energy density of MCA.[51] At the same time, the SOI is the important issue of the MCA.[51]

Actually, the validity of the expansion of $\rho_{ij}(\hat{\mathbf{M}})$ rather than $\rho_{ij}(\hat{\mathbf{H}})$ is not sure because most of the measurements are performed in a high applied magnetic field, which satisfy $\mathbf{M} \parallel \mathbf{H}$. If an unsaturated field is applied, the direction of **M** rather than **H** changes. It is reasonable to represent the variation of SCAMR by the expansion of $\rho_{ij}(\hat{\mathbf{M}})$ rather than $\rho_{ij}(\hat{\mathbf{H}})$, which has been used to determine the magnetic anisotropy.[54,55] Figure 3(a) shows the results of unsaturated SCAMR measured at 100 mT under different current directions relative to the EA. The significant deviation from the saturated result shown in Fig. 2(b) reveals the validity of our suggestion.

When we try to fit the experimental results in Fig. 3(a) with Eq. (3), it is necessary to obtain the angle of φ_M. Considering the Zeeman energy and cubic MCA energy, under the coherent rotation model, the total free energy density of the system can be expressed as

$$F = -\mu_0 M_s H\cos\alpha + \frac{1}{4}K\sin^2 2(\varphi_{EA}+\beta-\alpha), \quad (4)$$

where μ_0 is the vacuum permeability, M_s is the saturation magnetization, and K is the cubic MCA constant. $\varphi_M = \beta - \alpha$ can be derived by $\partial F/\partial\alpha = 0$ with small angle approximation

$$\varphi_M \approx \beta - \frac{\sin 4(\varphi_{EA}+\beta)}{4[h+\cos 4(\varphi_{EA}+\beta)]}, \quad (5)$$

where $h = H/H_K$ and $H_K = 2K/\mu_0 M_s$ is the effective cubic MCA field. This approach has been successfully used to analyze the conventional AMR.[52,54,55]

Figures 3(b) and 3(c) show the fitting results by Eq. (3) combined with Eq. (5) when **J** is along [110] and [100] directions, respectively. The 100 mT magnetic field ensures the validity of Eq. (5), under which the H is larger than twice of the anisotropy field of about 50 mT of the $Fe_{30}Co_{70}$ thin films and the magnetization process is coherent rotation rather than domain-wall motion or nucleation.[52] The purple curves in Figs. 3(b) and 3(c) represent the second term in Eq. (3), and the blue and green curves represent the third and fourth terms, respectively. Adopting the parameters $\rho_2 = 4.185 \times 10^{-2}\ \mu\Omega$ cm and $\rho_2^C = -7.337 \times 10^{-2}\ \mu\Omega$ cm under 6 T, it can be seen that the experimental data are fitted by the total results well. At the same time, $\rho_4^C = 4.460 \times 10^{-3}\ \mu\Omega$ cm and $H_K = 38$ mT along the EA are obtained. It shows that the magnitude of fourfold symmetry term ρ_4^C is almost one order of smaller than that of the twofold symmetry terms ρ_2 and ρ_2^C. Therefore, the fourfold symmetry of SCAMR is not obvious, in general, unless the two terms of the twofold symmetry are approximately equal and signs are opposite. In the $Fe_{30}Co_{70}$ films, the MCA-dependent twofold symmetry term ρ_2^C is larger than ρ_2, which

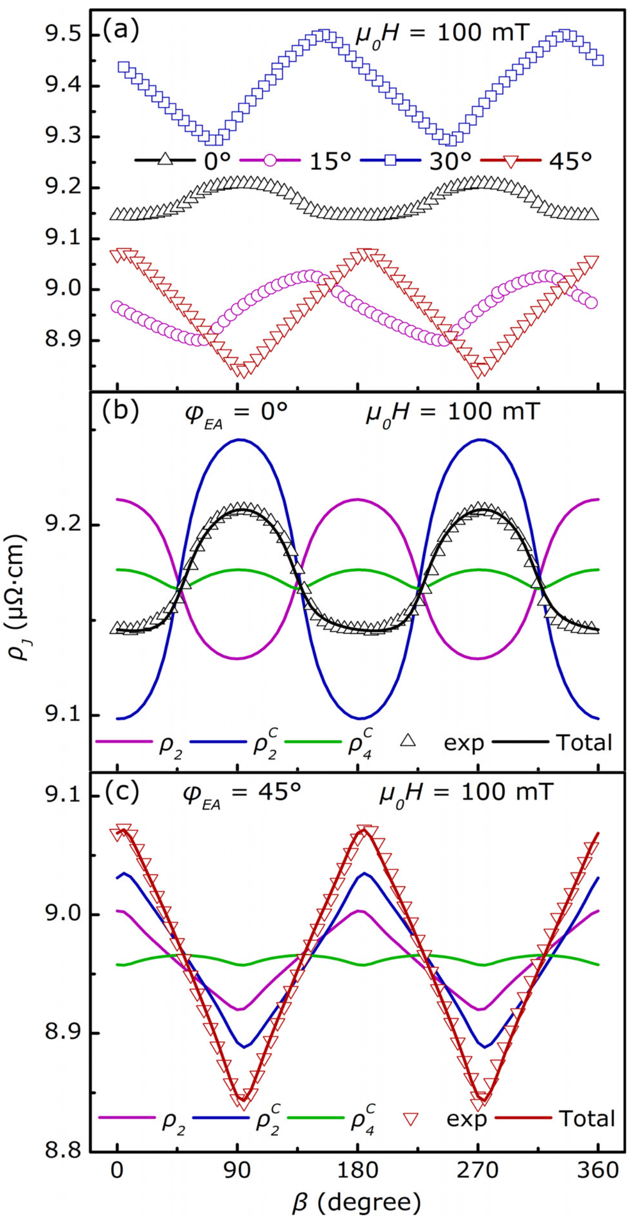

FIG. 3. (a) SCAMR as a function of β under 100 mT in different current directions with respect to the easy axis. The fitting results by Eq. (3) at (b) $\varphi_{EA} = 0°$ and (c) $\varphi_{EA} = 45°$. The open triangles are the experimental data. The purple solid lines represent MCA-independent SCAMR, while the blue and green solid lines represent twofold and fourfold symmetry MCA-dependent AMR, respectively.

ultimately dominates the phase-shift of SCAMR and leads to a negative SCAMR in the [110] crystallographic direction. This also causes the SCAMR ratio to have an order of magnitude difference in different crystallographic directions as reported in other systems,[26,31,32,56] but there is no negative SCAMR and significant phase-shift reported in ferromagnetic metals like Fe[26] and $Fe_{100-x}Co_x$ ($x \leq 65$).[56]

In order to verify the correctness of the effective MCA field obtained by fitting the SCAMR, Fig. 4 shows the frequency conversion

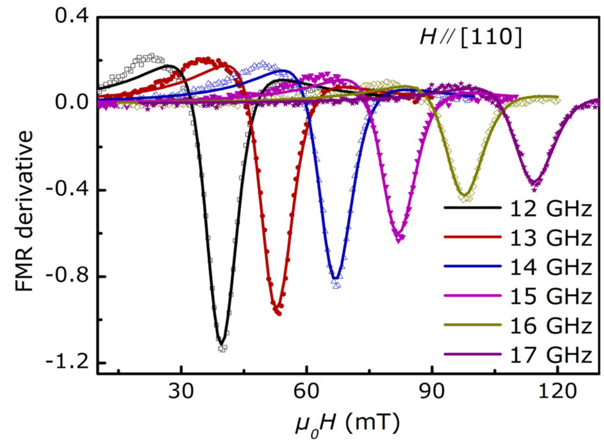

FIG. 4. The frequency conversion FMR spectra with the magnetic field applied along [110] crystallographic directions.

FMR results with the applied magnetic field along the EA [110] direction. The resonance field H_r can be obtained from the curves with different frequencies. It is known that a more general expression of the resonance frequency derived by Baselgia *et al.* is[57]

$$\left(\frac{\omega}{\gamma}\right)^2 = \frac{1}{M_s^2}\left[\frac{\partial^2 F}{\partial \theta^2}\left(\frac{1}{\sin^2\theta}\frac{\partial^2 F}{\partial \varphi^2} + \frac{\cos\theta}{\sin\theta}\frac{\partial F}{\partial \varphi}\right) - \left(\frac{1}{\sin\theta}\frac{\partial^2 F}{\partial\theta\partial\varphi} - \frac{\cos\theta}{\sin^2\theta}\frac{\partial F}{\partial\varphi}\right)\right], \tag{6}$$

where ω is the resonance frequency, γ is the gyromagnetic ratio, and θ and φ are the polar angle and azimuthal angle with respect to the EA direction, respectively. With $\theta = 90°$ and $\varphi = 0°$, the resonance frequency of a thin film with the EA along the x direction in the film plane can be obtained as an improved Kittel formula $\omega = \mu_0\gamma\sqrt{(M_s + H_K + H_r)(H_K + H_r)}$. For $Fe_{30}Co_{70}$ films, $H_K = 40$ mT at the EA is worked out by fitting the resonance field dependence of resonance frequency. This result corresponds to that obtained from the unsaturated SCAMR and reveals the reasonableness of Eq. (3) where the EA is the reference crystal axis.

At this point, we rewrite the SCAMR as

$$\Delta\rho_J = \rho_J(\varphi_M, \varphi_{EA}) - \rho_J(0, \varphi_{EA}). \tag{7}$$

In Eq. (7), the influence of crystalline resistance and device difference is ruled out as shown in Fig. 5(a), where the SCAMR of magnetization and the MCA is highlighted. It clearly shows the significant phase-shift of SCAMR and the sign change from negative AMR along [110] to positive AMR along [100]. Figure 5(b) shows the SCAMR at $\varphi_{EA} = 30°$ under different applied magnetic fields. It is found that there is almost no change with the increase in the field from 1 T to 9 T, which indicates further that the influence of the applied magnetic field on our results can be ignored. Correspondingly, with temperature decreasing, the H_K and ρ_2^C increase with a similar trend, which further proves the correlation between MCA and SCAMR (supplementary material III).

To conclude, we investigated the SCAMR of $Fe_{30}Co_{70}$ thin films on MgO(001) with current applied along different crystallographic

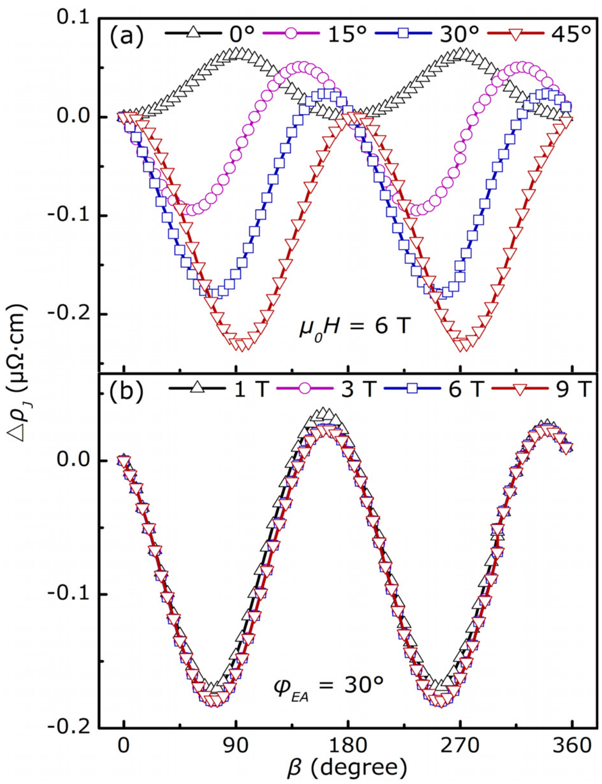

FIG. 5. (a) SCAMR ratios as a function of β under 6 T in different current directions with respect to the EA. (b) SCAMR ratios as a function of β under different applied magnetic fields at $\varphi_{EA} = 30°$.

directions. The SCAMR accompanied a huge phase-shift until its sign changes from negative to positive with the direction of the current applied from [110] to [100]. Under the MCA symmetry-adapted model, a more general SCAMR expression is derived by using the EA reference axis and is composed of a MCA-independent conventional term $\cos 2\varphi_M$ and a series of MCA-dependent terms $\cos 2n\varphi_A$ ($n \geq 1$), which describes the experimental results well under whatever the high or low magnetic field. We also verified the correctness of the SCAMR, in which the MCA-dependent twofold term contributes the negative AMR, which cannot be used as a fingerprint of the half-metallicity. This MCA symmetry-adapted SCAMR can provide an approach for the design and research of the magnetoresistance in the spin electronic devices, and the influence of symmetry-adapted MCA on the electrical transport properties can also be extended to analyze various Hall effects.

See the supplementary material for the sample growth, structural characterization, and the temperature dependence of the SCAMR of the $Fe_{30}Co_{70}$ films.

This work was supported by the National Natural Science Foundation of China (Grant Nos. 91963201, 11674143, and 11674141); 111 Project (B20063); and PCSIRT (Grant No. IRT 16R35).

DATA AVAILABILITY

The data that support the findings of this study are available within the article and its supplementary material.

REFERENCES

[1]W. Thomson, Proc. R. Soc. **8**, 546 (1857).
[2]E. Englert, Ann. Phys. **406**, 589 (1932).
[3]T. R. McGuire and R. I. Potter, IEEE Trans. Magn. **11**, 1018 (1975).
[4]T. R. McGuire, J. A. Aboaf, and E. Klokholm, J. Appl. Phys. **55**, 1951 (1984).
[5]W. Gil, D. Görlitz, M. Horisberger, and J. Kötzler, Phys. Rev. B **72**, 134401 (2005).
[6]H. C. V. Elst, Physica **25**, 708 (1959).
[7]T. R. McGuire, J. A. Aboaf, and E. Klokholm, IEEE Trans. Magn. **20**, 972 (1984).
[8]T. Endo, H. Kubota, and T. Miyazaki, J. Magn. Soc. Jpn. **23**, 1129 (1999).
[9]M. Tsunoda, Y. Komasaki, S. Kokado, S. Isogami, C.-C. Chen, and M. Takahashi, Appl. Phys. Express **2**, 083001 (2009).
[10]J. Smit, Physica **17**, 612 (1951).
[11]L. Berger, Physica **30**, 1141 (1964).
[12]R. I. Potter, Phys. Rev. B **10**, 4626 (1974).
[13]I. A. Campbell, A. Fert, and R. Pomeroy, Philos. Mag. **15**, 977 (1967).
[14]A. Fert and I. A. Campbell, Phys. Rev. Lett. **21**, 1190 (1968).
[15]I. A. Campbell, Phys. Rev. Lett. **24**, 269 (1970).
[16]I. A. Campbell, A. Fert, and O. Jaoul, J. Phys. C **3**, S95 (1970).
[17]O. Jaoul, I. Campbell, and A. Fert, J. Magn. Magn. Mater. **5**, 23 (1977).
[18]A. P. Malozemoff, Phys. Rev. B **32**, 6080 (1985).
[19]A. P. Malozemoff, Phys. Rev. B **34**, 1853 (1986).
[20]S. Kokado, M. Tsunoda, K. Harigaya, and A. Sakuma, J. Phys. Soc. Jpn. **81**, 024705 (2012).
[21]W. L. Webster, Proc. R. Soc. **113**, 196 (1926).
[22]R. Gans and J. v. Harlem, Ann. Phys. **407**, 516 (1932).
[23]L. Berger and S. A. Friedberg, Phys. Rev. **165**, 670 (1968).
[24]M. Tondra, D. K. Lottis, K. T. Riggs, Y. Chen, E. D. Dahlberg, and G. A. Prinz, J. Appl. Phys. **73**, 6393 (1993).
[25]R. P. van Gorkom, J. Caro, T. M. Klapwijk, and S. Radelaar, Phys. Rev. B **63**, 134432 (2001).
[26]F. Zeng, C. Zhou, M. Jia, D. Shi, Y. Huo, W. Zhang, and Y. Wu, J. Magn. Magn. Mater. **499**, 166204 (2020).
[27]X. Xiao, J. H. Liang, B. L. Chen, J. X. Li, D. H. Ma, Z. Ding, and Y. Z. Wu, J. Appl. Phys. **118**, 043908 (2015).
[28]X. Xiao, J. X. Li, Z. Ding, and Y. Z. Wu, J. Appl. Phys. **118**, 203905 (2015).
[29]N. Naftalis, A. Kaplan, M. Schultz, C. A. F. Vaz, J. A. Moyer, C. H. Ahn, and L. Klein, Phys. Rev. B **84**, 094441 (2011).
[30]M. Wang, C. Andrews, S. Reimers, O. J. Amin, P. Wadley, R. P. Campion, S. F. Poole, J. Felton, K. W. Edmonds, B. L. Gallagher, A. W. Rushforth, O. Makarovsky, K. Gas, M. Sawicki, D. Kriegner, J. Zubáč, K. Olejník, V. Novák, T. Jungwirth, M. Shahrokhvand, U. Zeitler, S. S. Dhesi, and F. Maccherozzi, Phys. Rev. B **101**, 094429 (2020).
[31]T. Sato, S. Kokado, M. Tsujikawa, T. Ogawa, S. Kosaka, M. Shirai, and M. Tsunoda, Appl. Phys. Express **12**, 103005 (2019).
[32]Y. Bason, J. Hoffman, C. H. Ahn, and L. Klein, Phys. Rev. B **79**, 092406 (2009).
[33]F. Takata, K. Kabara, K. Ito, M. Tsunoda, and T. Suemasu, J. Appl. Phys. **121**, 023903 (2017).
[34]A. W. Rushforth, A. D. Giddings, K. W. Edmonds, R. P. Campion, C. T. Foxon, and B. L. Gallagher, Phys. Status Solidi c **3**, 4078 (2006).
[35]A. W. Rushforth, K. Výborný, C. S. King, K. W. Edmonds, R. P. Campion, C. T. Foxon, J. Wunderlich, A. C. Irvine, P. Vašek, V. Novák, K. Olejník, J. Sinova, T. Jungwirth, and B. L. Gallagher, Phys. Rev. Lett. **99**, 147207 (2007).
[36]W. Döring, Ann. Phys. **424**, 259 (1938).
[37]P. K. Rout, I. Agireen, E. Maniv, M. Goldstein, and Y. Dagan, Phys. Rev. B **95**, 241107 (2017).
[38]A. Işin and R. V. Coleman, Phys. Rev. **142**, 372 (1966).
[39]R. Ramos, S. K. Arora, and I. V. Shvets, Phys. Rev. B **78**, 214402 (2008).

[40]J. Volný, D. Wagenknecht, J. Železný, P. Harcuba, E. Duverger-Nedellec, R. H. Colman, J. Kudrnovský, I. Turek, K. Uhlířová, and K. Výborný, Phys. Rev. Mater. **4**, 064403 (2020).
[41]A. Philippi-Kobs, A. Farhadi, L. Matheis, D. Lott, A. Chuvilin, and H. P. Oepen, Phys. Rev. Lett. **123**, 137201 (2019).
[42]R. R. Birss, *Symmetry and Magnetism* (North-Holland, Amsterdam, 1964).
[43]Q. Li, H. S. Wang, Y. F. Hu, and E. Wertz, J. Appl. Phys. **87**, 5573 (2000).
[44]M. Ziese, Phys. Rev. B **62**, 1044 (2000).
[45]J. O'Donnell, J. N. Eckstein, and M. S. Rzchowski, Appl. Phys. Lett. **76**, 218 (2000).
[46]X. Liu, W. Mi, Q. Zhang, and X. Zhang, Phys. Rev. B **96**, 214434 (2017).
[47]F. J. Yang, Y. Sakuraba, S. Kokado, Y. Kota, A. Sakuma, and K. Takanashi, Phys. Rev. B **86**, 020409 (2012).
[48]S. Tong, X. Zhao, D. Wei, and J. Zhao, Phys. Rev. B **101**, 184434 (2020).
[49]M. Tsunoda, H. Takahashi, S. Kokado, Y. Komasaki, A. Sakuma, and M. Takahashi, Appl. Phys. Express **3**, 113003 (2010).
[50]T. Hupfauer, A. Matosabiague, M. Gmitra, F. Schiller, J. Loher, D. Bougeard, C. H. Back, J. Fabian, and D. Weiss, Nat. Commun. **6**, 7374 (2015).
[51]S. Chikazumi, *Physics of Ferromagnetism* (Oxford University Press, 1997).
[52]Y. Miao, X. Chen, S. Yang, K. Zheng, Z. Lian, Y. Wang, P. Wang, C. Gao, D.-Z. Yang, and D.-S. Xue, J. Magn. Magn. Mater. **512**, 167013 (2020).
[53]E. D. Ranieri, A. W. Rushforth, K. Výborný, U. Rana, E. Ahmad, R. P. Campion, C. T. Foxon, B. L. Gallagher, A. C. Irvine, J. Wunderlich, and T. Jungwirth, New J. Phys. **10**, 065003 (2008).
[54]W. Limmer, M. Glunk, J. Daeubler, T. Hummel, W. Schoch, R. Sauer, C. Bihler, H. Huebl, M. S. Brandt, and S. T. B. Goennenwein, Phys. Rev. B **74**, 205205 (2006).
[55]W. Limmer, J. Daeubler, L. Dreher, M. Glunk, W. Schoch, S. Schwaiger, and R. Sauer, Phys. Rev. B **77**, 205210 (2008).
[56]F. L. Zeng, Z. Y. Ren, Y. Li, J. Y. Zeng, M. W. Jia, J. Miao, A. Hoffmann, W. Zhang, Y. Z. Wu, and Z. Yuan, Phys. Rev. Lett. **125**, 097201 (2020).
[57]L. Baselgia, M. Warden, F. Waldner, S. L. Hutton, J. E. Drumheller, Y. Q. He, P. E. Wigen, and M. Maryško, Phys. Rev. B **38**, 2237 (1988).